Assessment of spatial variability in soil models using centrifuge cone penetration tests

D.-H. Choi
Korea Advanced Institute of Science Technology, Daejeon, South Korea, donghyeong1105@kaist.ac.kr

T.-H. Kwon, S.-B. Lee, Y. Kang
Korea Advanced Institute of Science Technology, Daejeon, South Korea, t.kwon@kaist.ac.kr, lee_sb@kaist.ac.kr, sdthings0268@guest.kaist.ac.kr

J.-H. Kim
Kangwon National University, Chuncheon, South Korea, jaehyun2@kangwon.ac.kr

D. Kwak, D. Park
Hanyang University, Ansan/Seoul, South Korea, dkwak@hanyang.ac.kr, dpark@hanyang.ac.kr

Y. Lee, H.-S. Kim
Central Research Institute, Korea Hydro and Nuclear Power Co., Ltd., Daejeon, South Korea, dragon202@khnp.co.kr, haksung.kim@khnp.co.kr

ABSTRACT: The spatial variability is defined as the variation in soil properties across a spatial domain, driven by the inherent heterogeneity and geometric structures of soil formations resulting from diverse geological processes. Understanding spatial variability is critical, as it directly affects the reliability of foundation design, slope stability analyses, and other infrastructure-related assessments. The geotechnical centrifuge, a highly reliable testing method, can facilitate more realistic soil-structure-system design by enabling the assessment of spatial variability within soil models. The cone penetration test (CPT) has been utilized to assess spatial variability due to its ability to provide a continuous cone tip resistance (q_c) profile during penetration. Prior studies have quantified spatial variability using the coefficient of variation (*CV*) and the scale of fluctuation or correlation length (*CL*). However, q_c alone is limited in its direct applicability to geotechnical design. This study investigated the spatial variability of soil properties using centrifuge CPT data, with a focus on the influence of gravitational acceleration (*g-level*) on spatial variability assessments. The results demonstrate that q_c-based spatial variability is significantly influenced by *g-level*, with *CV* decreasing and *CL* increasing as *g-level* rises, particularly in dense soil states. This study advances geotechnical engineering by using centrifuge-based CPT to assess spatial variability, enhancing realistic design through q_c and V_s measurements across diverse soil conditions.

1 INTRODUCTION

The inherent heterogeneity of natural soils results in spatial variability of their properties, which profoundly affects the design and performance of geotechnical structures, thereby influencing the overall reliability and safety of these systems. (Rathje et al., 2010; Stewart & Afshari, 2021; Chala & Ray, 2025).

Random field theory offers a solid approach for representing this variability, treating spatially fluctuating soil properties as probabilistic models that account for their intricate and frequently anisotropic characteristics. Phoon & Kulhawy (1999) highlighted that random fields incorporate spatial correlation patterns, effectively managing uncertainty in engineering designs. Essential for reliability-based approaches in such scenarios is the measurement of this variability via metrics like the coefficient of variation (*CV*) and the correlation length (*CL*, also referred to as the scale of fluctuation, SoF) (Cao & Wang, 2013).

In assessing spatial variability on-site, the cone penetration test (CPT) combined with statistical and geostatistical techniques is employed to determine parameters such as *CV* and *CL*. The CPT delivers almost continuous, detailed profiles of soil attributes, including cone tip resistance (q_c), sleeve friction (f_s), and pore water pressure, facilitating in-depth evaluation of stratified and non-uniform deposits for assessing soil liquefaction or the site response analysis

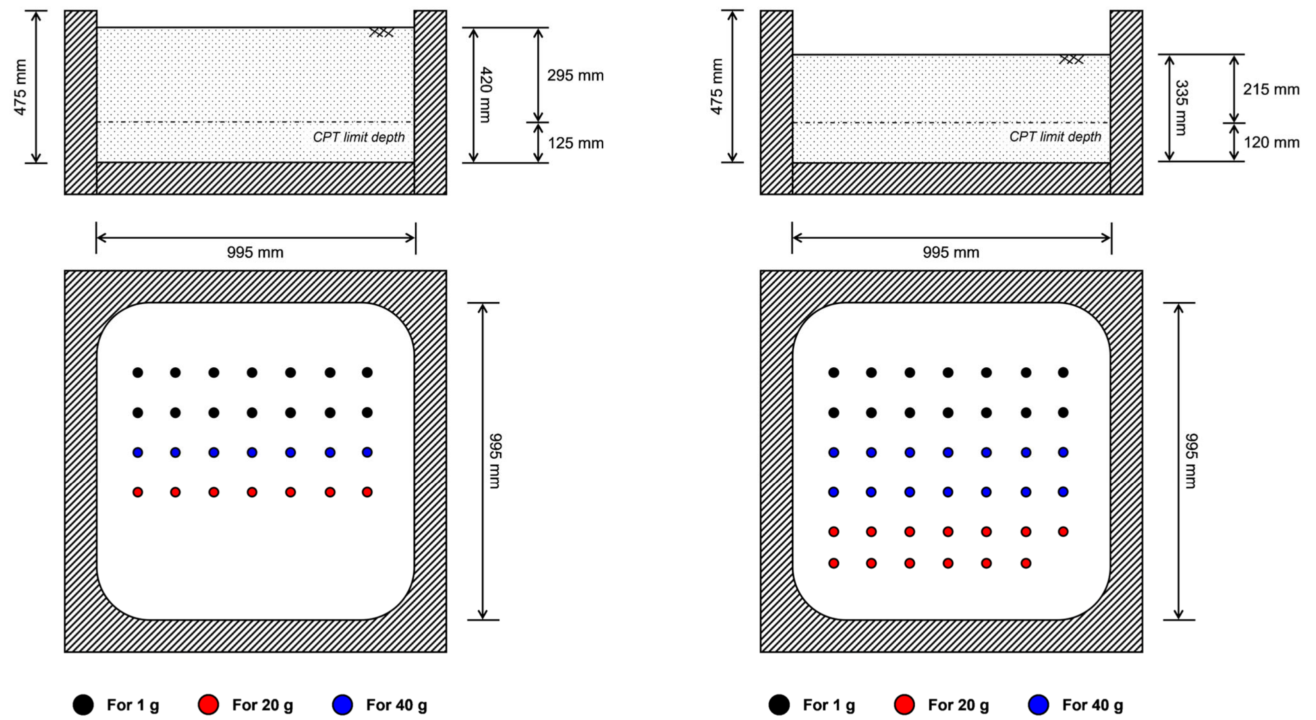

Figure 1. Soil model layouts: (a) T1-SP81: dry silica sand, (b) T2-SM98: dry weathered soil.

(Juang et al., 2003; Cao & Wang, 2013; Stamati et al., 2016; Amjadi & Johari, 2022). Nevertheless, obstacles arise from the expensive data acquisition process, resulting in limited datasets, presumptions of stationarity and isotropy that might not apply to anisotropic materials, and the intensive computational requirements for extensive simulations (Phoon & Kulhawy, 1999; Cao & Wang, 2013).

Geotechnical centrifuge tests offer unique benefits in overcoming on-site constraints by recreating the stress field in a controlled laboratory setting, enabling systematic parametric investigations under reduced-scale scenarios that mimic real-world phenomena (Madabhushi, 2017). It's noteworthy that most physical modeling studies assume the soil model is homogeneous when filled inside a container. However, in practice, it can be heterogeneous across spatial locations and scales, even though the soil model comprises a single soil type. It's necessary to assess the extent of this heterogeneity.

Although progress has been made in describing spatial variability in soils, several research deficiencies remain that limit the accuracy and applicability of current models. 1) Although research has explored spatial variability in specific geotechnical parameters, there is insufficient understanding of whether this variability differs according to the type of parameter. For example, comparisons between parameters such as q_c and shear wave velocity (V_s) are rare, which could impede a comprehensive evaluation of how the unique characteristics of these parameters impact spatial heterogeneity. 2) The role of confining stress in shaping spatial variability has not been thoroughly investigated, leading to ambiguities regarding how varying stress states alter the extent and configuration of soil variability under diverse loading scenarios.

To bridge these shortcomings, this study presents an approach for emulating different soil conditions employing reduced-scale physical replicas in a centrifuge, assessing spatial variability using CPT data. More specifically, we investigate spatial variability among various soil models by means of centrifuge CPTs and q_c-V_s conversion approaches. To examine the effects of confining stress, centrifuge CPTs are carried out under three different gravitational acceleration (*g-level*, *g*) conditions.

2 TEST CONFIGURATION

2.1 Soil models

To examine spatial variability across diverse soil conditions, the present investigation developed two distinct soil models, designated as T1-SP81 and T2-SM98 (Fig. 1). These models were assembled within a rigid rectangular container with internal dimensions of 995 mm in both length and width, and 475 mm in height. Each model incorporated a uniform soil material: dry silica sand for T1-SP81 and dry weathered soil for T2-SM98, thereby ensuring consistency in intrinsic properties within each respective configuration. The T1-SP81 model was constructed to a height of 420 mm, whereas T2-SM98 was prepared to a height of 335 mm, accommodating variations in experimental parameters such as stress distributions or penetration depths. The median particle diameter (d_{50}) was determined to be 0.236 mm for the silica sand and 0.874 mm for the weathered soil. Soil preparation involved meticulously controlled compaction to attain the targeted relative density (D_r), with initial values recorded at 81.8% for T1-SP81 and 98.8% for T2-SM98. Per the Unified Soil Classification System (USCS), T1-SP81 was categorized as SP (poorly graded sand), while T2-SM98 was classified as SM (silty sand).

2.2 Cone penetration test

A miniature cone with a diameter of 12 mm was used, equipped with a Wheatstone-bridge load cell comprising four strain gauges to measure the q_c accurately. The CPTs were conducted at three g-levels—1 *g*, 20 *g*, and 40 *g*—to simulate different stress conditions for T1-SP81 and T2-SM98. The exact locations of the CPTs are detailed in Fig. 1, with tests conducted at 1 *g* at locations marked in black, 20 *g* at locations marked in red, and 40 *g* at locations marked in blue, ensuring a systematic distribution to capture spatial variability. All For T1-SP81, a total of 28 CPTs were performed upto 295 mm depth: 14 at 1 *g*, 7 at 20 *g*, and 7 at 40 *g*. For T2-SM98, 41 CPTs were conducted upto 215 mm depth: 14 at 1 *g*, 13 at 20 *g*, and 14 at 40 *g*. Furthermore, to ensure reliable and comparable results, all CPTs adhered to conditions established in prior studies that minimize influences on cone penetration resistance (Gui et al., 1998; Bolton et al., 1999; Kim et al., 2016).

3 TEST RESULTS

3.1 Cone penetration test

The q_c obtained from the CPTs was plotted against the prototype depth, scaled according to the applied g-levels, also considering radial effect, for two soil models, T1-SP81 and T2-SM98, as shown in Fig. 2. A notable observation is that CPT profiles conducted at lower stress levels (*i.e.*, lower *g-levels*) exhibited higher cone tip resistance at shallow penetration depths. This finding aligns with the conclusions of Bałachowski (2007), who reported that when CPTs are performed at different centrifugal accelerations using a single cone diameter, the combined effects of particle size and stress level significantly influence the results.

However, contrary to the findings of Kim et al. (2016), who suggested that the *g-level* effect on cone penetration resistance becomes more pronounced with higher D_r, this study observed a less pronounced

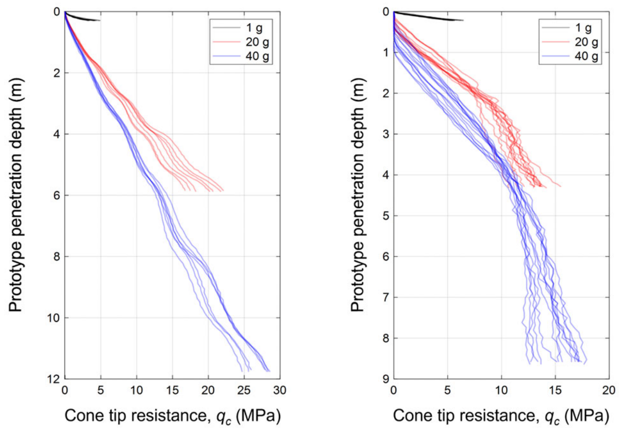

Figure 2. CPT results under different g-level conditions: (a) T1-SP81, (b) T2-SM98.

difference in T2-SM98, even though it has a higher relative density (D_r = 98.81%) compared to T1-SP81 (D_r = 81.81%). This discrepancy may be related to the soil dilatancy characteristics highlighted by Kim et al. (2016), particularly in dense sands. Unlike T1-SP81, which is classified as poorly graded sand (SP), T2-SM98 contains approximately 12% fine content, leading to its classification as silty sand (SM).

Previous studies have indicated that dilatancy significantly decreases for silty sands like T2-SM98 as the fine content exceeds a critical threshold. Specifically, increased interparticle interactions can enhance dilatancy when the fine content is low (< 7%). However, as the fine content increases beyond 7% and approaches 20%, dilatancy markedly decreases, likely because fine particles hinder interparticle interactions and restrict volumetric expansion during the application of shear stress (Xiao et al., 2014).

4 ANALYSIS AND DISCUSSION

4.1 q_c-V_s conversion

The q_c-V_s conversion is performed following the procedures proposed in previous studies and was as follows (Liao & Whitman, 1986; Robertson et al., 1992; Boulanger, 2003; Moss et al., 2006):

$$V_{s1} = V_s \cdot (P_a/\sigma'_v)^{0.25} \tag{1a}$$

$$V_{s1} = Y \cdot (q_{c1})^a \tag{1b}$$

$$q_{c1} = C_N \cdot q_c \tag{1c}$$

$$C_N = (P_a/\sigma'_v)^n \tag{1d}$$

where V_{s1} is the normalized V_s (m/s), q_{c1} is the normalized q_c (MPa), C_N is the normalizing factor, σ_v' is the vertical effective stress (MPa), P_a is the atmospheric pressure (MPa), Y, a, and n are empirical constants. By collectively considering Eqs. 1a, 1b, 1c, and 1d, the expression can be developed into a single equation as follows:

$$V_s = A \cdot \left(P_a/\sigma_v'\right)^B \cdot q_c^C \tag{2}$$

where V_s is the shear wave velocity obtained from the resonant column test, P_a/σ_v' is calculated from the soil unit weight, q_c is the cone tip resistance measured from CPT, and A, B, C are the empirical constants which are determined from regression analysis using the least-squares method (Choi, 2025).

4.2 Spatial variability assessment

This section examines the roles of the CV, CL, and the autocorrelation fitting method (ACFM) in quantifying the spatial variability of soil. The CV is a dimensionless, non-directive measure of relative variability, defined as the ratio of the standard deviation (σ) to the mean (μ) of a soil property (*i.e.*, $CV = \sigma/\mu$). A high CV indicates significant variability, which can increase risks such as differential settlement or slope instability (Vanmarcke, 1977). The CL represents the distance over which a soil property remains correlated, reflecting the spatial "wavelength" of variability. Smaller CL values suggest rapid fluctuations, necessitating denser sampling, while larger CL values indicate gradual changes. Vanmarcke (1977) noted that CL is different in vertical and horizontal directions, reflecting anisotropic soil conditions, so that vertical directional CL (CL_v) and horizontal directional CL (CL_h) are analyzed separately in this study. To calculate the CL, the coefficient of correlation (ρ) can be calculated with the separation distance (τ) as follows:

$$\rho(\tau) = \frac{\sum_{h=0}^{\tau max-\tau-1}(V_{s,h}-\bar{V_s})(V_{s,h+\tau}-\bar{V_s})}{\sum_{h=0}^{\tau max-\tau-1}(V_{s,h}-\bar{V_s})^2} \tag{3}$$

where $V_{s,h}$ and $V_{s,h+t}$ is a pair of shear wave velocities where the separation distance between the two points is τ, $\bar{V_s}$ is the mean shear wave velocity of the pair. Then the $\rho(\tau)$, the CL (θ), can be calculated as:

$$\theta = \int_{-\infty}^{\infty} \rho(\tau)\ d\tau = 2\int_0^{\infty} \rho(\tau)\ d\tau \tag{4}$$

The autocorrelation fitting method ($ACFM$) is widely used to estimate CL with fitting theoretical autocorrelation models, such as the Markovian (Eq. 5a) and the Gaussian (Eq. 5b) models to the sample autocorrelation function, $\rho(\tau)$, calculated as (Vanmarcke, 1977, 1983, 2010):

$$\rho(\tau) = exp(-2|\tau|/\theta) \tag{5a}$$

$$\rho(\tau) = exp\{-\pi(|\tau|/\theta)^2\} \tag{5b}$$

Soil properties often exhibit systematic trends with depth (e.g., increasing density), violating the stationarity assumption required for $ACFM$. The detrending process removes these trends to ensure data stationarity, enabling accurate autocorrelation analysis. Vanmarcke (1977) suggested standardizing data to remove depth-dependent trends, such as transforming original depth-dependent parameter $u(z)$ to detrended parameter $u_{dt}(z) = [u(z)- \bar{u}(z)] / \bar{u}(z)$, where $\bar{u}(z)$ is the mean profile of $u(z)$. However, the issue is that most previous studies in geotechnical engineering do not either provide detailed explanations of the detrending methods employed or arbitrarily assume a linear mean profile (Vanmarcke, 1977; Fenton, 1999; Nie et al., 2015) (Fig. 3a).

Such approaches result in a critical limitation: the stationary condition of the data is not maintained after detrending. Unfortunately, previous studies directly addressing depth-related detrending in $ACFM$ are scarce, indicating a research gap. The application of the linear detrending method presents a limitation, as it may lead to overestimation in cases of highly variable q_c profiles. A literature review indicates that the quadratic detrending method results in a reduced correlation distance compared to linear detrending (Sasanian et al., 2019). While quadratic detrending can mitigate the overestimation of correlation distance inherent in linear detrending, it may also result in overestimation for profiles with significant variability. Consequently, there is a need to develop methods to address these limitations and enhance the accuracy of spatial variability assessments.

To address this issue, a new detrending method is proposed by adapting the moving average technique, commonly used in hydrology and physics to remove fluctuations from long-term trends (Alessio et al., 2002; Carbone et al., 2004a & 2004b), as follows:

$$u_{dt}(z) = u(z) - \bar{u}_{mavg}(w) \tag{6a}$$

$$0.9 \times u(z) \le u_{dt}(z) \le 1.1 \times u(z) \tag{6b}$$

where $u_{dt}(z)$ is the detrended V_s profile, $u(z)$ is the original V_s profile, $\bar{u}_{mavg}(z)$ is the moving averaged mean profile, and w is the size of the window for

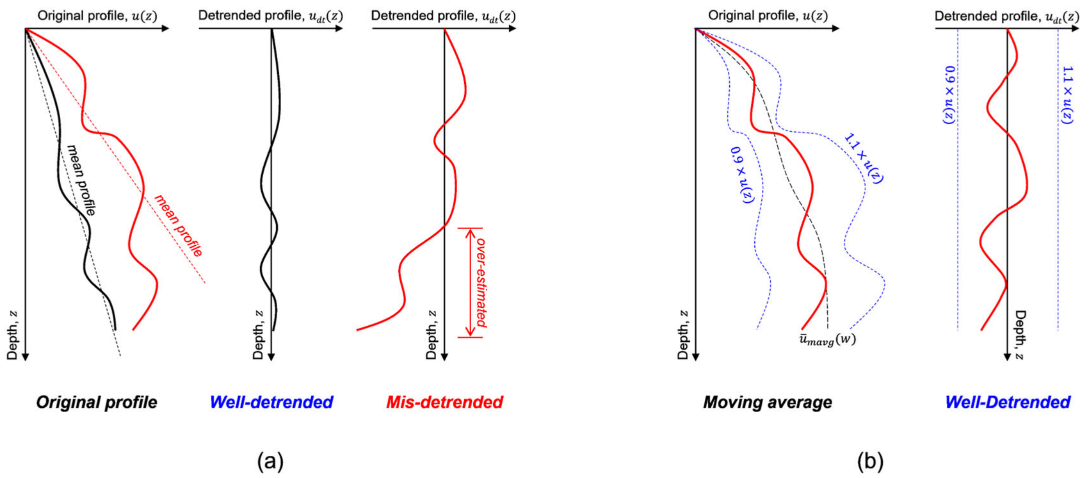

Figure 3. Conceptual diagrams of detrending process: (a) conventional detrending case using linear mean profile, (b) newly suggested moving average detrending method.

moving averaging, 20% length of $u(z)$ used for w in this study (Fig. 3b). However, the w can be changed if it satisfies the conditions described in Eq. 6*b*.

The spatial variability of soil models T1-SP81 and T2-SM98 was analyzed based on previously outlined procedures, with results summarized in Table 1. The analysis evaluated spatial variability using q_c and V_s independently, revealing distinct outcomes (Figs. 4 & 5). For instance, under 1 g conditions for T1-SP81, the CV for q_c was 0.957, with a vertical correlation length CL_v of 0.1088 m and a horizontal correlation length CL_h of 0.6787 m, based on a Markovian model. To evaluate the percentage of how much the CL reaches the maximum CL, the normalized CL, vertical and horizontal correlation length ratios (R_{CLv} and R_{CLh}) are calculated as follows:

$$R_{CL_v} = CL_v / max(CL_v) \tag{7a}$$

$$R_{CL_h} = CL_h / max(CL_h) \tag{7b}$$

When normalized against the maximum CL, these values correspond to 36.3% and 2.0%, respectively. In contrast, for V_s, the CV was 0.269, with CL_v of 0.0061 m and CL_h of 0.72 m. These differences are attributed to the correlation process between V_s and q_c-derived parameters via the resonant column test. Notably, CL_h consistently equaled the maximum CL across all cases, likely due to an insufficiently small sampling interval, which limited the data available for accurate CL_h estimation (Nie et al., 2015).

4.3 g-level effect on spatial variability

To investigate the influence of *g-level* on spatial variability, CV, R_{CLv}, and R_{CLh} were compared across different g-levels (Fig. 6). The spatial variability based on q_c decreased as the g-level increased, while CV and R_{CLv} decreased, and R_{CLh} remained at its maximum value in T1-SP81 (Table 1). This trend was consistent in T2-SM98, and the CV and R_{CLv} decreased with increasing g-level. However, in the case of the V_s analysis, both T1-SP81 and T2-SM98 showed almost no changes in CV with increasing g-level, and R_{CLv} exhibited very low values across all g-levels. This pattern was also observed in T2-SM98.

The variation in spatial variability with increasing g-level exhibits a complex pattern when assessed using q_c. Specifically, the CV decreases, while the characteristic CL_v increases, with the extent of these changes varying depending on the soil model. This behavior is attributed to the observation that the rate of increase in q_c with penetration depth becomes more pronounced at lower *g-levels* (Fig. 2).

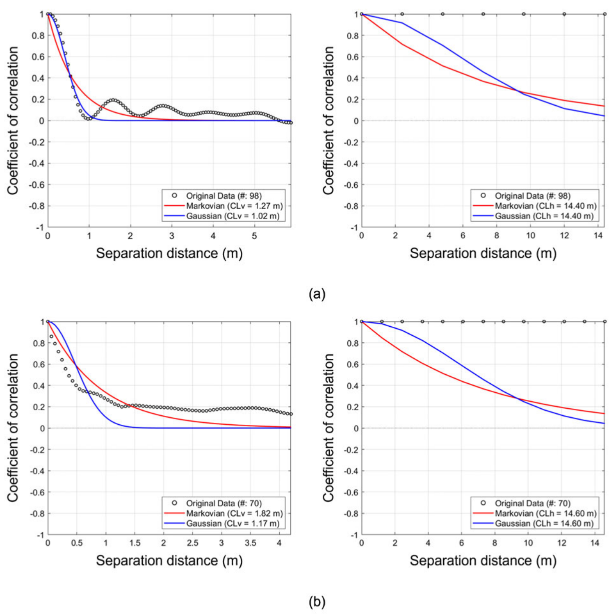

Figure 4. One of the q_c-based correlation length results at 20 g-level: (a) T1-SP81, (b) T2-SM98.

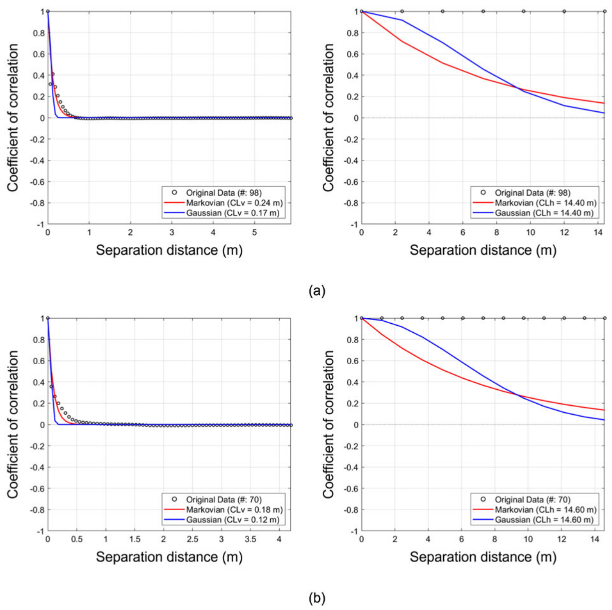

Figure 5. One of the V_s-based correlation length results at 20 g-level: (a) T1-SP81, (b) T2-SM98.

In contrast, when spatial variability is evaluated using V_s, the rate of increase in V_s relative to penetration depth remains consistent across different *g-levels*, resulting in no discernible *g-level*-dependent differences in spatial variability. Consequently, when evaluating spatial variability using q_c, the influence of *g-level* effects must be considered. To minimize the impact of *g-level* variations when comparing the spatial variability of soil models under different *g-levels*, it is recommended to convert q_c measurements to V_s for evaluation. However, caution is advised when assessing soils with low relative density, as *g-level* effects may be less pronounced in such cases (Kim et al., 2016).

5 CONCLUSIONS

This study investigated the spatial variability of soil properties using centrifuge CPT data, with a focus on the influence of gravitational acceleration, saturation conditions, and relative density on spatial variability assessments. The analysis utilized two soil models, T1-SP81 (dry silica sand) and T2-SM98 (dry weathered soil), to evaluate spatial variability through statistical parameters such as the *CV* and *CL*. The findings highlight the complex interplay between soil conditions, testing methodologies, and spatial variability outcomes.

The results demonstrate that q_c-based spatial variability is significantly influenced by *g-level*, with *CV* decreasing and R_{CLv} increasing as g-level rises, particularly in dense soil states. This *g-level* effect is attributed to the pronounced increase in q_c with penetration depth at lower g-levels, as observed in T1-SP81 and T2-SM98. In contrast, V_s-based spatial variability exhibited negligible g-level dependency, with consistent *CV* and R_{CLv} values across all g-levels. This suggests that V_s provides a more stable measure of spatial variability unaffected by gravitational scaling. Consequently, converting q_c to V_s is recommended to minimize *g-level* effects when comparing spatial variability across different stress conditions, although caution is advised for low relative density soils where *g-level* effects may be less pronounced.

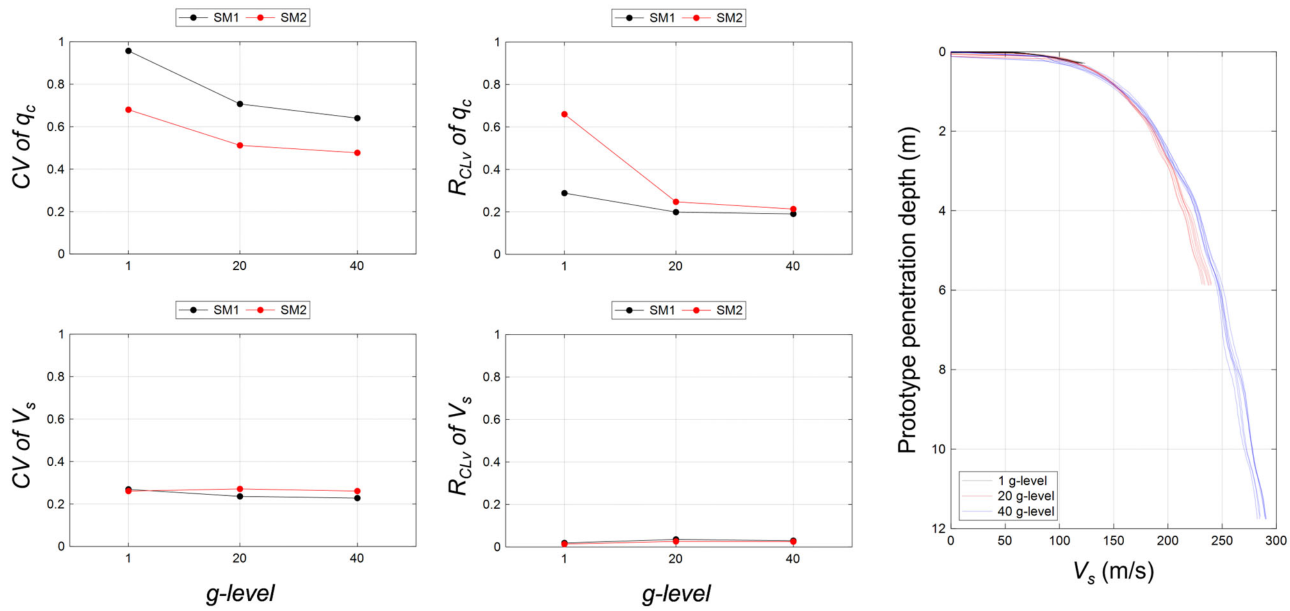

Figure 6. g-level effect on spatial variability: (a) CV, (b) R_{CLv}, (c) V_s profiles of T1-SP81.

Table 1. Spatial variability of T1-SP81 and T2-SM98.

T1-SP81							
g-level	**Index property**	**AFCM**	**Max.**	q_c	q_c-R_{CL}	V_s	V_s-R_{CL}
1 g	*CV*	-	-	0.957	-	0.269	-
	CL_v (m)	Markovian	0.3	0.1088	36.3%	0.0061	2.0%
		Gaussian		0.0865	28.8%	0.0057	1.9%
	CL_h (m)	Markovian	0.72	0.6787	93.0%	0.7299	100.0%
		Gaussian		0.6803	93.2%	0.7299	100.0%
20 g	*CV*	-	-	0.707	-	0.236	-
	CL_v (m)	Markovian	6	1.7014	28.4%	0.2545	4.2%
		Gaussian		1.1934	19.9%	0.2144	3.6%
	CL_h (m)	Markovian	14.4	14.4	100.0%	14.4	100.0%
		Gaussian		14.4	100.0%	14.4	100.0%
40 g	*CV*	-	-	0.640	-	0.228	-
	CL_v (m)	Markovian	12	3.0004	25.0%	0.5026	4.2%
		Gaussian		2.2861	19.1%	0.3561	3.0%
	CL_h (m)	Markovian	28.8	28.8	100.0%	28.8	100.0%
		Gaussian		28.8	100.0%	28.8	100.0%
T2-SM98							
g-level	**Index property**	**AFCM**	**Max.**	q_c	q_c-R_{CL}	V_s	V_s-R_{CL}
1 g	*CV*	-	-	0.512	-	0.271	-
	CL_v (m)	Markovian	0.21	0.1765	84.0%	0.0019	0.9%
		Gaussian		0.1386	66.0%	0.0029	1.4%
	CL_h (m)	Markovian	0.72	0.72	100.0%	0.72	100.0%
		Gaussian		0.72	100.0%	0.72	100.0%
20 g	*CV*	-	-	0.512	-	0.271	-
	CL_v (m)	Markovian	4.2	1.4565	34.7%	0.1502	3.6%
		Gaussian		1.0388	24.7%	0.1111	2.6%
	CL_h (m)	Markovian	14.6	14.6	100.0%	14.6	100.0%
		Gaussian		14.6	100.0%	14.6	100.0%
40 g	*CV*	-	-	0.477	-	0.261	-
	CL_v (m)	Markovian	8.4	2.2919	27.3%	0.3028	3.6%
		Gaussian		1.7923	21.3%	0.2135	2.5%
	CL_h (m)	Markovian	28.8	28.8	100.0%	28.8	100.0%
		Gaussian		28.8	100.0%	28.8	100.0%

ACKNOWLEDGEMENTS

The project presented in this paper is supported by Korea Hydro and Nuclear Power Co., Ltd. (KHNP) and by the National Research Foundation of Korea (NRF) grant funded by the Korean government (MSIT)(RS-2024-00340851).

REFERENCES

Alessio, E., Carbone, A. N. N. A., Castelli, G., & Frappietro, V. (2002). Second-order moving average and scaling of stochastic time series. The European Physical Journal B-Condensed Matter and Complex Systems, 27(2), 197-200. https://doi.org/10.1140/epjb/e20020150

Amjadi, A. H., & Johari, A. (2022). Stochastic nonlinear ground response analysis considering existing boreholes locations by the geostatistical method. Bulletin of Earthquake Engineering, 20(5), 2285-2327. https://doi.org/10.1007/s10518-022-01322-1

Bałachowski, L. (2007). Size effect in centrifuge cone penetration tests. Archives of Hydro-Engineering and Environmental Mechanics, 54(3), 161-181.

Bolton, M. D., Gui, M. W., Garnier, J., Corte, J. F., Bagge, G., Laue, J., & Renzi, R. (1999). Centrifuge cone penetration tests in sand. Géotechnique, 49(4), 543-552. https://doi.org/10.1680/geot.1999.49.4.543

Boulanger, R. W. (2003). High overburden stress effects in liquefaction analyses. Journal of geotechnical and geoenvironmental engineering, 129(12), 1071-1082. https://doi.org/10.1061/(ASCE)1090-0241(2003)129:12(1071)

Cao, Z., & Wang, Y. (2013). Bayesian approach for probabilistic site characterization using cone penetration tests. Journal of Geotechnical and Geoenvironmental Engineering, 139(2), 267-276. https://doi.org/10.1061/(ASCE)GT.1943-5606.0000765

Carbone, A., Castelli, G., & Stanley, H. E. (2004a). Analysis of clusters formed by the moving average of a long-range correlated time series. Physical Review E, 69(2), 026105. https://doi.org/10.1103/PhysRevE.69.026105

Carbone, A., Castelli, G., & Stanley, H. E. (2004b). Time-dependent Hurst exponent in financial time series. Physica A: Statistical Mechanics and its Applications, 344(1-2), 267-271. https://doi.org/10.1016/j.physa.2004.06.130

Chala, A., & Ray, R. Efficient Uncertainty Quantification in Seismic Site Response via Random Field Modeling. In Geotechnical Frontiers 2025 (pp. 158-169). https://doi.org/10.1061/9780784485996.016

Choi, D. -H. (2025). Assessment of Spatial Variability and Seismic Ground Motion Incoherency of Soil Deposits in Physical Modeling. Ph.D. Thesis, Department of Civil and Environmental Engineering, KAIST, Republic of Korea.

Fenton, G. A. (1999). Random field modeling of CPT data. Journal of geotechnical and geoenvironmental engineering, 125(6), 486-498. https://doi.org/10.1061/(ASCE)1090-0241(1999)125:6(486)

Gui, M. W., & Bolton, M. D. (1998). Geometry and scale effects in CPT and pile design. In Geotechnical site characterization (pp. 1063-1068).

Juang, C. H., Yuan, H., Lee, D. H., & Lin, P. S. (2003). Simplified cone penetration test-based method for evaluating liquefaction resistance of soils. Journal of geotechnical and geoenvironmental engineering, 129(1), 66-80. https://doi.org/10.1061/(ASCE)1090-0241(2003)129:1(66)

Kim, J. H., Choo, Y. W., Kim, D. J., & Kim, D. S. (2016). Miniature cone tip resistance on sand in a centrifuge. Journal of Geotechnical and Geoenvironmental Engineering, 142(3), 04015090. https://doi.org/10.1061/(ASCE)GT.1943-5606.0001425

Liao, S. S., & Whitman, R. V. (1986). Overburden correction factors for SPT in sand. Journal of geotechnical engineering, 112(3), 373-377. https://doi.org/10.1061/(ASCE)0733-9410(1986)112:3(373)

Madabhushi, G. (2017). Centrifuge modelling for civil engineers. CRC press. https://doi.org/10.1201/9781315272863

Moss, R. E., Seed, R. B., & Olsen, R. S. (2006). Normalizing the CPT for overburden stress. Journal of Geotechnical and Geoenvironmental Engineering, 132(3), 378-387. https://doi.org/10.1061/(ASCE)1090-0241(2006)132:3(378)

Nie, X., Zhang, J., Huang, H., Liu, Z., & Lacasse, S. (2015). Scale of fluctuation for geotechnical probabilistic analysis. In Geotechnical safety and risk V (pp. 834-840). IOS Press. https://doi.org/10.3233/978-1-61499-580-7-834

Phoon, K. K., & Kulhawy, F. H. (1999). Characterization of geotechnical variability. Canadian geotechnical journal, 36(4), 612-624. https://doi.org/10.1139/t99-038

Rathje, E. M., Kottke, A. R., & Trent, W. L. (2010). Influence of input motion and site property variabilities on seismic site response analysis. Journal of geotechnical and geoenvironmental engineering, 136(4), 607-619. https://doi.org/10.1061/(ASCE)GT.1943-5606.000025

Robertson, P. K., Woeller, D. J., & Finn, W. D. L. (1992). Seismic cone penetration test for evaluating liquefaction potential under cyclic loading. Canadian Geotechnical Journal, 29(4), 686-695. https://doi.org/10.1139/t92-075

Sasanian, S., Soroush, A., & Jamshidi Chenari, R. (2019). Effect of sampling interval on the scale of fluctuation of CPT profiles representing random fields. International Journal of Civil Engineering, 17, 871-880. https://doi.org/10.1007/s40999-018-0371-3

Stamati, O., Klimis, N., & Lazaridis, T. (2016). Evidence of complex site effects and soil non-linearity numerically estimated by 2D vs 1D seismic response analyses in the city of Xanthi. Soil Dynamics and Earthquake Engineering, 87, 101-115. https://doi.org/10.1016/j.soildyn.2016.05.006

Stewart, J. P., & Afshari, K. (2021). Epistemic uncertainty in site response as derived from one-dimensional ground response analyses. Journal of Geotechnical and Geoenvironmental Engineering, 147(1), 04020146. https://doi.org/10.1061/(ASCE)GT.1943-5606.0002402

Vanmarcke, E. (2010). Random fields: analysis and synthesis.

Vanmarcke, E. H. (1977). Probabilistic modeling of soil profiles. Journal of the geotechnical engineering division, 103(11), 1227-1246. https://doi.org/10.1061/AJGEB6.0000517

Vanmarcke, E.H. (1983). Random fields: analysis and synthesis. MIT press, Cambridge, pp 247-264. https://doi.org/10.1029/EO064i037p00550

Xiao, Y., Liu, H., Chen, Y., & Chu, J. (2014). Strength and dilatancy of silty sand. Journal of Geotechnical and Geoenvironmental Engineering, 140(7), 06014007. https://doi.org/10.1061/(ASCE)GT.1943-5606.0001136